Malaysian Journal of Civil Engineering 22(2) : 264-290 (2010)

SEISMIC PERFORMANCE OF BEAM-COLUMN JOINTS IN REINFORCED CONCRETE BUILDINGS SUBJECTED TO REVERSIBLE VERTICAL CYCLIC LOADING

Nor Hayati Abdul Hamid[1]

[1] *Faculty of Civil Engineering, Univesiti Teknologi MARA, 40450, Shah Alam, Selangor, Malaysia*

Abstract: Three identical half-scale of exterior beam-column joints of RC buildings with different arrangement of connections detailing are designed, constructed and tested under reversible vertical cyclic loading. Each set consists of reinforced concrete beams, column and foundation beam which represents the exterior joints of the ground floor of RC buildings. The objectives of this study are to examine seismic performance, to observe visual damages and to classify different types of damages which occur in beam-column joints. The first set is designed beam-column joint in accordance to BS 8110 where no anchorages of bars are tied between beam and column. Second set comprises of three anchorage bars from column are placed and tied with top of reinforcement bars in the beam. Third set is designed with cross-bracing of reinforcement bars at the intersection of beam-column joint. Results showed that the beam-column connections which designed according to BS 8110 without anchorage bars suffer the most severe damages as compared to connections with anchorage bars and cross-bracing bars. Beam-column joint with cross-bracing bars experienced less damage as compared to two types of joints. Visual structural damages of beam-column joints include cracks prorogation, the spalling of concrete shell, buckling of longitudinal reinforcement bars and fractured of shear reinforcement bars. Therefore, it is an appropriate time to revise and replace the current code of practice to seismic code so that reinforced concrete buildings which are constructed in Malaysia are save under long-distant earthquake excitation and local earthquake.

Keywords: beam-column joint, vertical cyclic loading, damages, spalling of concrete, visual observation

1.0 Introduction

The seismic performance of reinforced concrete buildings in high, medium and low seismic regions need to be examined carefully. Detailing of the point of intersection in RC buildings where the load is transferred from one structural component to another structural component such as beam-column joint, wall-foundation joint and slab-beam joint must be carefully designed. Particular

attention should be focused on arrangement of reinforcement bars at joints, spacing and arrangement of the links. Compressive strength of concrete, detailing of beam-column joints and workmanship play an important role in assessing the seismic performance under seismic loading (Paulay et al., 1978). Beam-column joint is defined as the zone of intersection between beams and columns with the functional requirement which enable the adjoining members to develop and sustain their ultimate capacity. The joint should provide sufficient strength and endurance to resist the internal forces transferred by the framing members.

Basically, there are three types of beam-column joints which are interior joint, exterior joint and corner joint (Uma and Meher, 2002). This study focuses on the design, construction and testing exterior beam-column joint at ground level under quasi-static vertical cyclic loading. At ground level of beam-column joint, all the loads which include dead, imposed, wind and earthquake loadings are meet and transfer to the foundation beam. Therefore, the exterior beam-column joints at ground floor are considered critical joints and require investigating their performance under loading combination. Consequently, three identical half-scale beam-column joints with three types of joint arrangements are constructed, calibrated and tested in heavy structural laboratory. These types of connections together with their individual foundation beam are clamped to strong floor before testing under vertical cyclic loading. Mode of failures, spalling of concrete, buckling of longitudinal reinforcement bars and fractured of shear reinforcement bars are among the damages that can be observed during experimental work. Identification and classification of damages are based on the visual damages, percentage of drift, cracking pattern, buckling of reinforcement bars and spalling of concrete cover. Further nonlinear dynamic analysis can be modeled based on the load versus displacement (hysteresis loop), stress-strain relationship and crack propagation.

2.0 Structural Damages Following Past Earthquakes

A beam-column joint is the crucial zone in reinforced concrete buildings where vertical loading and lateral loading are met and transfer their load to the foundation. This type of joint has high risk of failures as compared to others structural components when an earthquake strikes at any areas in seismic regions where this is the possibility of occurrence of plastic-hinge zone mechanism. Failure of beam-column joints in RC buildings was identified as one of the leading causes of collapse during earthquake which classified them as soft-story mechanism (strong beam and column weak). Figure 1 shows the joint failure due to poor detailing and workmanship which lead to the collapse of the structure

during the 2003 Boumerdes Earthquake. The damages are due to no diagonal reinforcement bars in the joint and spacing between links are wider which contribute to the failure of structures under earthquake attack (Alcocer and Carranza, 2002).

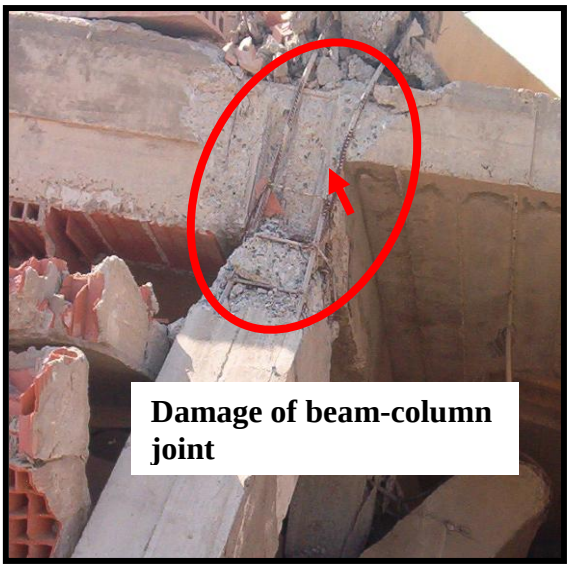

Figure 1: Seismic deficiency weak beam-column joint during the 2003 Boumerdes Earthquake.

Figure 2 shows two examples of damages occurred in beam-column joints after earthquake disasters. Figure 2(a) illustrates the cracks and spalling of nominal concrete cover at beam-column joints of at ground floor of five-storey reinforced concrete building during the 2001 Bhuj Earthquake, India. This is due to disorganization of beam-column joint and insufficient of longitudinal and shears reinforcement in the concrete. Figure 2(b) shows the severe damage of exterior beam-column joints during the 2001 Bhuj Earthquake due to instability of column where the spalling of concrete and buckling of reinforcement bars (Telford, 1996). Poor workmanship and lacking of detailing are among the factor that causes this type of damage on reinforced concrete structures when earthquake strike.

Figure 3 shows the spalling of nominal concrete cover in beam-column joints following an earthquake. The damage is due to insufficient stirrups which produce unconfined concrete and buckling of reinforcement at the intersection of beam-column joints. However, this damage can be repaired and strengthened by jacketing method around the column and joint.

Figure 2: Beam-column joint damages during the 2001 Bhuj Earthquake India ; (a) Disorganization of a beam to column joint is inadequate; and (b) Overloading of exterior beam-column joints.and lacking of stirrups.

Figure 3: Spalling of concrete cover at beam-column joints in reinforced concrete building.

Based the pictures' illustrations and problem arise in beam-column joint, the main objective of this paper is to improve the seismic performance of beam-column joint by using different types of arrangement of reinforcement bars at beam-column joints. Three sets of specimens were designed, constructed and tested under quasi-static vertical cyclic loading until collapse. Anchorage reinforcement bars are arranged in different orientation in order to improve the structural performance and strengthening the connection by avoiding soft-storey mechanism which expected to occur in the ground column. Three set sub-assemblage of half-scale beam-column joint together with foundation beam were designed in accordance to BS8110, constructed and tested in Heavy Structural Laboratory, Faculty of Civil Engineering, Universiti Teknologi MARA, Shah Alam, Selangor. Figure 4 shows the prototype of the exterior beam-column joint of reinforced concrete building of Block 1, Faculty of Civil Engineering, UiTM, Shah Alam, Selangor. However due to the space limitation, only one beam connected to column is constructed in the laboratory.

Figure 4: A prototype of exterior beam-column joint of ground floor of Block 1, Faculty of Civil Engineering, Universiti Teknologi MARA, Shah Alam, Selangor.

3.0 Monolithic Beam Analogy

In monolithic beam analogy, the member compatibility condition is used where the force in tension is equivalent to force in the compression by considering the stress-strain relationship in concrete and reinforcement bars. The stress-strain relationship is adopted for the concrete by assuming the simplified stress block by solving two unknowns which are the position of neutral axis and the strain in the concrete. The relationship between these global parameters is defined by introducing an analogy in term of global displacement by equating the displacement in precast connection with monolithic connection.

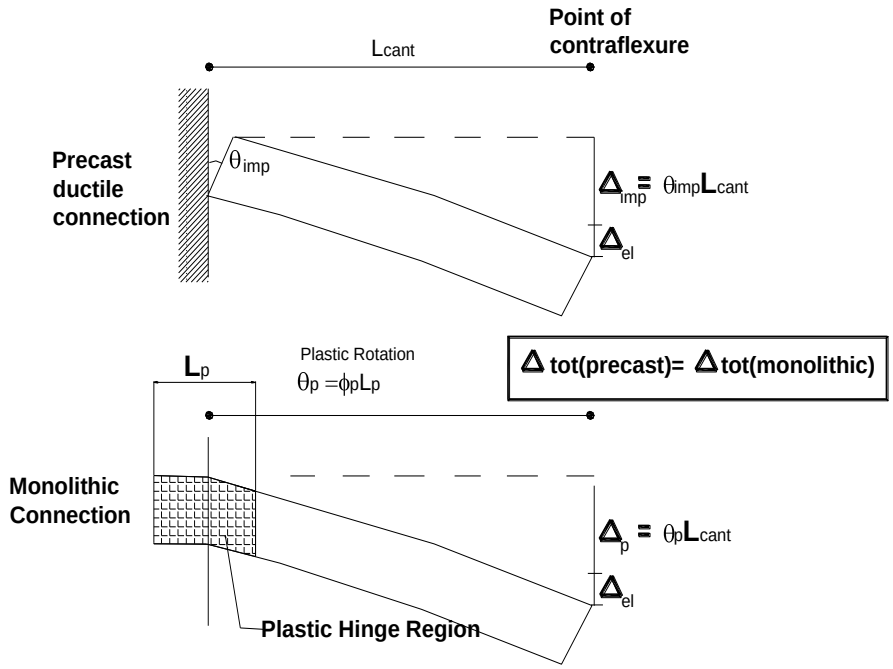

Figure 5: Monolithic beam analogy

Figure 5 shows the monolithic beam analogy for the beam-column connection. By assuming the point of contraflexure occurring in the beam due to lateral loads at mid-span and the end displacement of two different cantilever schemes are compared with each other. In precast ductile connection, the opening gap of the beam-column interface will result in an imposed rigid

rotation (θ_{imp}). The contribution to the total beam-edge displacement is due to a rigid rotation which can be derived as follows:

$$\Delta_{imp} = \theta_{imp} L_{cant} \tag{1}$$

Where L_{cant} is the distance between the interface and point of contraflexure. By adding the contribution due to elastic deformation, the total displacement of the precast beam is given by the following equation:

$$\Delta_{total\,(precast)} = \Delta_{imp} + \Delta_{elastic} \tag{2}$$

In the monolithic cantilever beam, the total displacement is the sum of elastic and plastic contribution where the latter approximated is given by the rigid rotation about the end of the beam (or the plastic hinge centroid).

$$\Delta_{total\,(monolithic)} = \Delta_{plastic} + \Delta_{elastic} \tag{3}$$

By assuming the two beams are identical in terms of geometry and reinforcement, the elastic deformations would be the same and when imposing the same total displacement, the 'plastic' contributions can be equated. In ductile precast connections, the inelastic deformation is localized at the interface while in monolithic beam is distributed along the plastic hinge. Hence, the equation becomes:

$$\Delta_{total\,(precast)} = \Delta_{total\,(monolithic)} \tag{4}$$

$$\Delta_{imp} + \Delta_{elastic} = \Delta_{plastic} + \Delta_{elastic} \tag{5}$$

By utilizing the monolithic case for ultimate and yielding curvature concepts introduced by Paulay and Priestley (1975):

$$\Delta_{plastic} = \theta_p (L_{cant} - \frac{L_p}{2}) = (\phi_u - \phi_y) L_p (L_{cant} - \frac{L_p}{2}) \tag{6}$$

Where L_p is the plastic hinge length in the monolithic beam. By combining Equation 5 and Equation 6, the above equation becomes:

$$\theta_p L_{cant} = (\phi_u - \phi_y) L_p (L_{cant} - \frac{L_p}{2}) \tag{7}$$

$$(\phi_u - \phi_y) = \frac{(\theta_{imp} L_{cant})}{(L_{cant} - \frac{L_p}{2}) L_p} \tag{8}$$

$$\phi_u = \frac{\varepsilon_c}{c} = \frac{(\theta_{imp} L_{cant})}{(L_{cant} - \frac{L_p}{2}) L_p} + \theta_y \tag{9}$$

$$\varepsilon_c = (\frac{(\theta_{imp} L_{cant})}{(L_{cant} - \frac{L_p}{2}) L_p} + \theta_y).c \tag{10}$$

By introducing additional condition on the global member displacement satisfies the member compatibility and results in a simple relationship between concrete strain and neutral axis position. For each guessed value of concrete strain, the member compatibility relationship provides a unique value of concrete strain, which should satisfy section equilibrium considerations. If the local equilibrium is violated a different value of neutral axis depth c should guessed, resulting in a trial and error procedure to find the real value. The whole procedure of plotting the graph of moment-rotation and load-deflection are described in the following section:

4.0 Procedure For Moment-Rotation Analysis For Ductile Connections

In the first stage of procedure moment-rotation analysis of beam-column connections is to perform trial and error guess by assuming the simplified hypotheses on the stress-strain distribution of concrete, stress-strain of reinforcement bars and member compatibility condition. The concept of "monolithic beam analogy" is used to evaluate the moment-rotation and load-displacement of beam-column joints in reinforced concrete buildings. The procedures for moment-rotation analysis for ductile connections in beam-column joints for reinforced concrete buildings are as follows:

Step 1: Fix the beam end rotation

The effective rotation (θ_b) developed at the beam-column interface due to the opening of the crack and it can be related to the drift frame system with simple geometric considerations as shown in Figure 6. The relationship between effective rotation (θ_b) and column rotation (θ) is given by the following equation:

$$\theta_b = \frac{\theta}{\left(1 - \frac{h_c}{L}\right)} \tag{11}$$

Step 2: Guess an initial neutral axis depth c for the beam

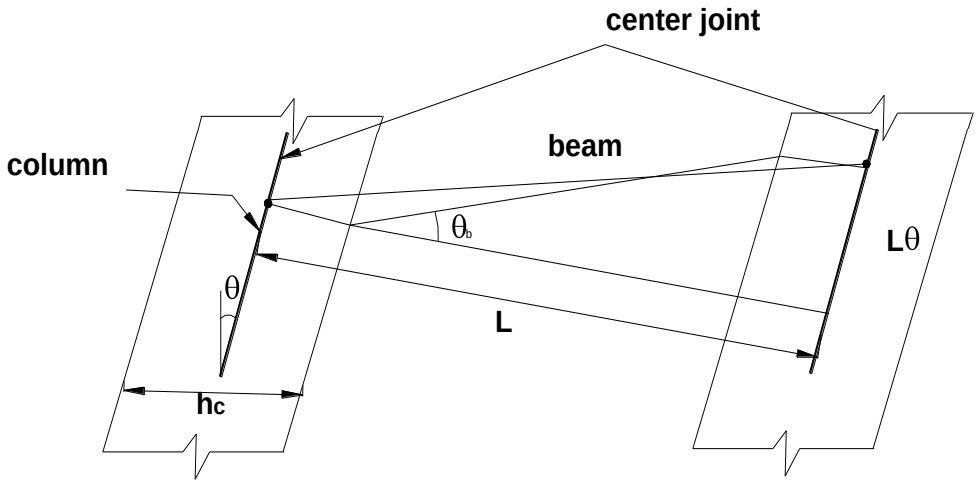

Figure 6: Interstorey drift-beam rotation relationship

Step 3: Evaluate the strain in reinforcement bars

The increase in the strain in the reinforcement bars is due to the beam deformation is taken into account the length and elongation of reinforcement bars. The strain of the reinforcement bar is given below:

$$\varepsilon_{pt} = \frac{n.\Delta_{pt}}{\left(\quad_{ub}\right)} \tag{12}$$

where $n=$ number of total openings along the beam (at beam-column interfaces), $l_{ub}=$ length of reinforcement bars in the beam-column interfaces, $\Delta_{pt}=$ elongation (elastic + plastic) at the level of the reinforcement bars.

$$\Delta_{pt}=\theta.\left(\frac{h}{2}-c\right) \tag{13}$$

where $\left(\frac{h}{2}-c\right)$ is the relative position of the reinforcement bars (assumed to be at mid-height of the section) and h is the beam height.

Step 4: Estimate in the mild steel and concrete

A strain compatibility cannot be adopted in order to relate the strain in the mild steel and high yield steel which should be separately evaluated referring to the deformation of all the beam member (member compatibility). In this case the concentrate of the rotation at the beam-column interface due to the opening of the crack simplifies the procedure. The strain in the steel can be estimates as:

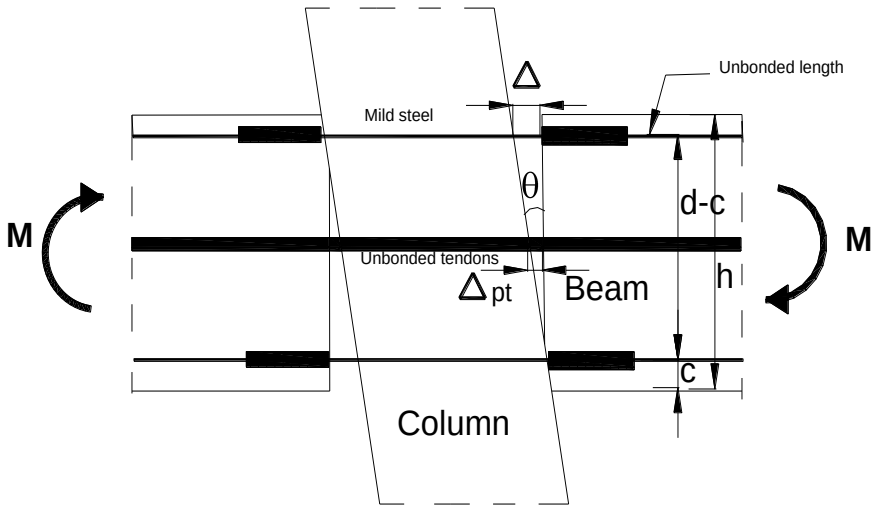

Figure 7: Gap opening mechanism

$$\varepsilon_s = \left(\frac{\Delta - 2\Delta_{sp}}{l_{ub}} \right) \tag{14}$$

where $\Delta =$ elongation at the level of the mild steel due to the opening of crack, $\Delta_{sp} =$ displacement due to strain penetration. $l_{ub} =$ unbonded length of the mild steel. For the mild steel, the strain penetration is assumed to occur at both ends of the unbonded region. The total extension reinforcement at the interface crack is:

$$\Delta = \theta.(d - c) \tag{15}$$

where $d =$ beam section depth. Contribution in displacement Δ due to strain penetration may be obtained using the procedure outlined in Sritharan (1998):

$$\Delta_{sp} = \frac{2}{3} l_{sp} \varepsilon_e + l_{sp} \varepsilon_p \tag{16}$$

where $l_{sp} =$ strain penetration taken as $0.15 f_y d_{bl}$; $f_y =$ yield strength of reinforcement; $d_{bl} =$ diameter of reinforcement bar; $\varepsilon_e =$ elastic strain in the beam reinforcement $\varepsilon_p =$ plastic strain in beam reinforcement. By substituting $\varepsilon_p = \varepsilon_s - \varepsilon_e$ and $\varepsilon_e = \alpha \varepsilon_y$ in Equation 14, the value of ε_s can be found using the following equation:

$$\varepsilon_s = \frac{\Delta - (4/3 l_{sp} \alpha \varepsilon_y - 2 l_{sp} \alpha \varepsilon_y)}{(l_{ub} + 2 l_{sp})} \tag{17}$$

which can be simplified into:

$$\varepsilon_s = \frac{\Delta + (2/3 l_{sp} \alpha \varepsilon_y)}{(l_{ub} + 2 l_{sp})} \tag{18}$$

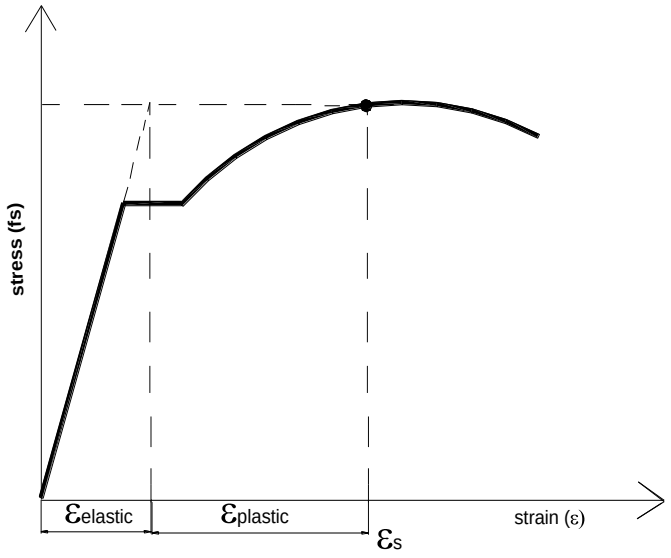

Figure 8: Elastic and plastic strain components

Following the estimation of the strain in the steel, the strain in the concrete should be derived with an accurate relationship that can no longer rely on the classical linear distribution hypothesis. If assuming a correct complete stress-strain relationship for the concrete, the problem would consist of a system of the two unknowns, namely the neutral axis depth c and the concrete strain ε_c. Two equations should thus be introduced by the section equilibrium and a sort of member compatibility. At this stage, a triangular or rectangular stress-block assumption can be provided an acceptable approximation. There is no calculation of ε_c and the procedure is reduced to a trial and error iteration on the unique unknown, *c*.

Step 5: Section equilibrium: new value of neutral axis depth 'c'

The compression resultant in the concrete is calculated from equilibrium considerations as the section as specify in Equation 19 :

$$C + T_s + C'_s = T_{pt} \tag{19}$$

where the compressive reinforcement force acting as an external force (T_{pt}) is given by the sum of the initial reinforcement bars (T_{in}) and the increment due to the deformation of the beam.

$$T_{pt} = T_{in} + f(\varepsilon_{pt})A_{pt} \tag{20}$$

where ε_{pt} = the elongation of the reinforcement bars, $f(\varepsilon_{pt})$ = the tensile stress in the reinforcement bars sue to their elongation. The neutral axis depth *(c)* is then derived from the compression resultant in the concrete, *C*, depending on the hypotheses on the stress-strain behaviour of the concrete. A simplified approach can be derived by assuming an equivalent stress block to represent distribution of stress in concrete.

Step 6: Iterative procedure until convergence

The iteration on the neutral axis depth *(c)* is therefore carried out until convergence. Rigorously, the initial hypotheses on the relation between the elastic and plastic components in the reinforcement strain (ε_{pt}) based on the values of the constant $\alpha(\varepsilon_e = \alpha\varepsilon_y)$ should cross-checked. Therefore few "double" iteration on (*c)* and α should be performed to reach convergence on both the parameters. It should be noted that updating α is important at small level of strains (thus at small level of rotation-drift) and becomes negligible at higher levels when entering the plastic domain.

Step 7: Evaluate the Moment Capacity

The moment resistance capacity of the section M, corresponding to the fixed rotation can be obtained by taking moment about an axis (such as through the mid-height of the section). The graph of moment capacity versus rotation can be plotted in order to compare with the experimental results.

Step 8: Determine the Load versus Displacement

The final step is to plot the graph load versus displacement based on the moment versus rotation as described in Step 7. Then, experimental result will be compared with theoretical results in order to find the correlation between them. In order to validate between theoretical results and experimental results, the sub-assemblage 3 sets of half-scale beam-column connections were constructed and tested under vertical cyclic loading. The next section will describe the construction of half-scale beam-column connections in heavy structures laboratory.

5.0 Construction Of The Specimens

After predicting the theoretical result of the beam-column connection, it is important to validate the experimental result with the theoretical results. Initially, the beam-column joints together with their foundation beams were assembled and constructed in heavy structural laboratory, Faculty of Civil Engineering, Universiti Teknologi MARA, Shah Alam, Selangor. The reinforcement bars cages for beam-column connections and foundation beam are prepared separately. Figure 9(a) shows the reinforcement bar cages for beam-column joints with 300mm spacing of stirrup within the six longitudinal reinforcement bars. Figure 9(b) shows the reinforcement bars cages for foundation beam with PVC pipes were inserted into bottom of the plywood. This hole is used to insert highly threaded rod to clamp the foundation to the strong floor. The beam-column cage is placed at the center of the foundation beam and tied it to the bottom reinforcement bar in foundation beam. This connection is similar as pile cap as designed for medium high-rise buildings.

Figure 10 shows the schematic arrangement of reinforcement bars in beam and detail connection between beam and column. Accurate measurement and arrangement of reinforcement bars in beam-column and column-foundation connection are very important before pouring the concrete. Figure 10(a) shows the bottom parts of column reinforcement bars which are overlapping to the foundation beam. Proper connections work and good workmanship contribute to the strength and stability of the buildings during earthquake attack. Figure 10(b) shows the location of PVC pipes attached to bottom plywood before pouring of concrete take place.

Figure 9: Construction of beam-column connection; (a) schematic arrangement of links in beam; and (b) location of PVC pipes in foundation beam before pouring concrete.

Figure 11 shows the detail connection between beam-column connections which will be tested in the laboratory under vertical cyclic loading to imitate the earthquake motion in vertical direction. Figure 11(a) shows detail connection using BS 8110 where there is no additional links of stirrup in the connection. The overlapping of reinforcement bars are placed in side the links of the column. This type of connection is normally used in most of the construction of reinforced concrete buildings in Malaysia. Figure 11(b) shows the cross-bracing of reinforcement bars inside the links and these links are tied together with longitudinal reinforcement bars of the column. Additional reinforcement bars were connected between top of beam to the longitudinal bars in column. This type of connection can transmit the lateral force from the beam to the column and finally to the foundation.

(a) (b)

Figure 10: Detailing of reinforcement bars in each specimen; (a) connections detailing between column and foundation ; and (b) beam and column caging of reinforcement bar.

Figure 12 shows the process of concreting for foundation beam using ready-mix concrete with compressive strength of 30MPa. The caging of foundation beam is placed into formwork before concreting take place. Figure 12(a) shows the ready-mix concrete is poured into the foundation beam and vibrator is used to make sure that the concrete has a proper compaction before hardening and avoid the formation of honeycomb in the concrete. Figure 12(b) shows the process of pouring concrete up to top level of foundation beam. The wet concrete was

poured up to the level of PVC pipe and the hole of PVC must be closed with plastic to avoid the concrete running through the hole. When concreting finished, the top part of the foundation beam must be covered with wet rugs for curing process take place otherwise creep, shortening and the surface crack will occur.

(a) Specimen 1

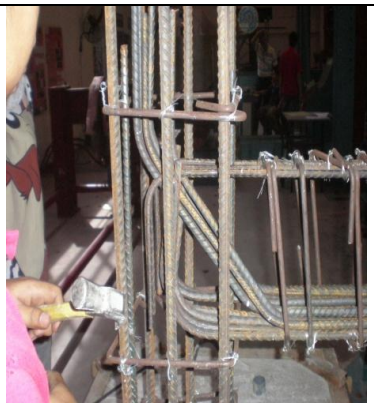

(b) Specimen 2

(c) Specimen 1

Figure 11: Connection detailing in beam-column connection; (a) Connection of Specimen 1; (b) Connection of Specimen 2; and (c) Connection of Specimen 3.

(a)

(b)

Figure 12: Process of concreting for foundation beam; (a) pouring concrete into the formwork of foundation beam; and (b) leveling top part of foundation beam up to PVC pipe.

After 3 days of curing, formwork can be dismantled and it is ready for testing. Figure 13 shows the isometric view of the specimen before testing. Foundation beam is clamped to strong floor using high-yield threaded rods so that it did not move during testing under vertical cyclic loading test. This specimen is ready for instrumentation and testing under vertical cyclic loading.

Figure 13: Foundation beam is clamped to strong floor using high-yield threaded rod.

6.0 Experimental Set-Up

Before experimental testing, five linear potentiometers were installed along the beam and column to measure the deformation under vertical cyclic loading. A total number of six strain gauges were attached to longitudinal reinforcement bars in beam and column to measure stress-strain relationship under cyclic loading. Figure 14 shows the five schematic locations of LVDT and six strain gauges in the beam and column.

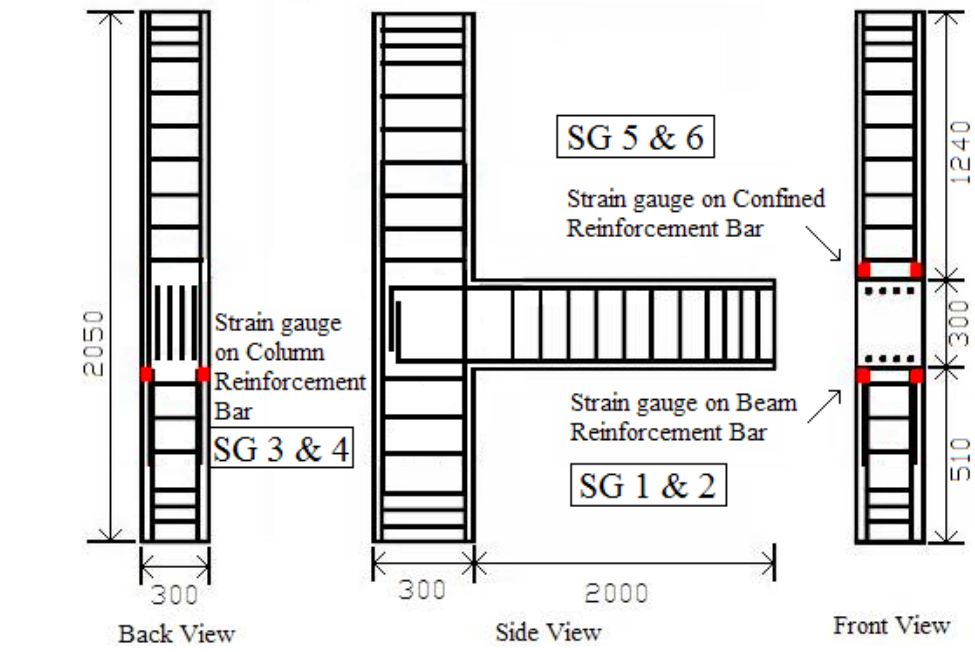

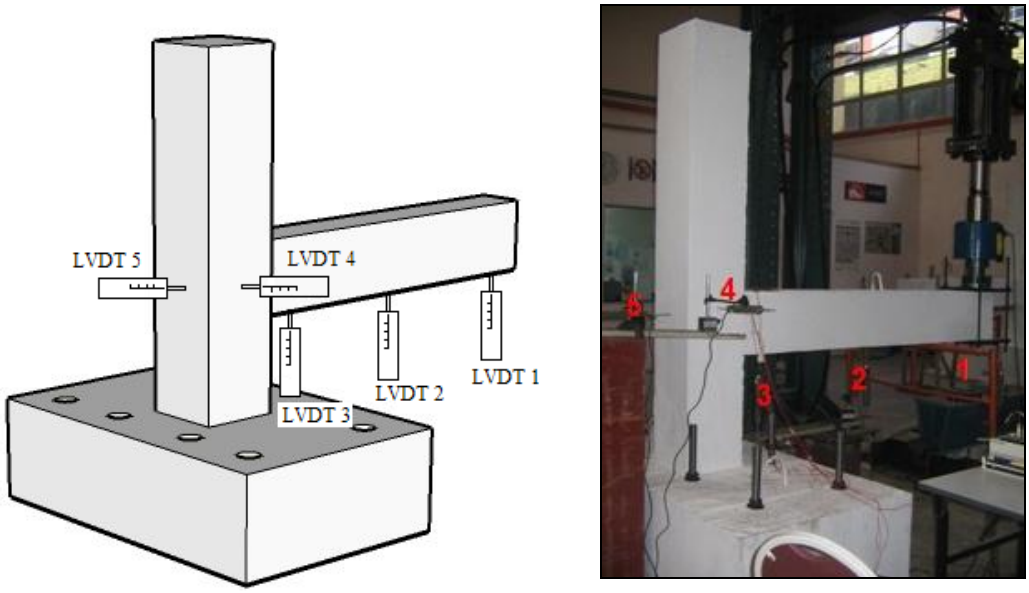

Figure 14: Schematic locations of strain gauges and LVDT along the beam and column.

7.0 Visual Observation On Beam-Column Damage

Figure 15 exhibits the visual observation of Specimen 1 which designed according to BS 8110 without any anchorages of reinforcement bars in the joints at 3% drift. Most of the diagonal cracks concentrated at joints and spalling of concrete cover at top surface of column (see Figure 15(a)). Diagonal cracks were occurred at middle of intersection of beam-column starting from top to bottom of the joints and spread down to the bottom of column (see Figure 15(b) and (c)).

(a) (b) (c)

Figure 15: Visual observation on the damage of Specimen 1; (a) spalling of concrete on surface of column ; (b) diagonal cracks from top to bottom of column; and (c) spalling and cracking of concrete cover of column.

Figure 16 illustrates the visual damage on Specimen 2 with three anchorage reinforcement bars are placed at top of beam and connected to the reinforcement bar in column. Specimen 2 has lesser damage as compared to the connection which designed according to BS 8110, namely Specimen 1. Based on visual observation, the upper part of beam is stronger than bottom part of beam due increase of percentage of steel in concrete. Figure 16(a), (b) and (c) show the progress development of cracks at the intersection starting from 1% drift to 3% drift. It can be concluded that this type joint in Specimen 2 has better seismic performance as compared to the joint in Specimen 1.

Figure 17 shows the visual damages which occurred on Specimen 3 with cross-bracing of anchorage bars from top to bottom of the link. This type of connection

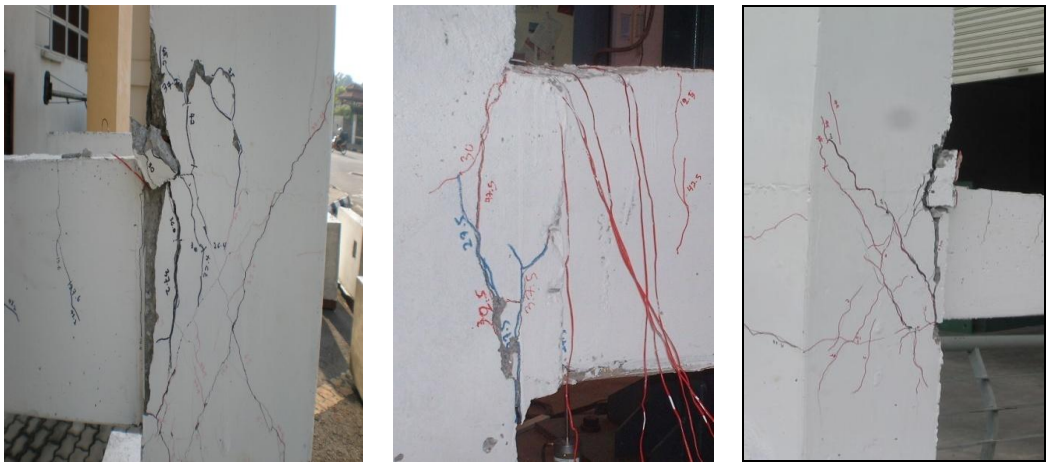

(a) (b) (c)

Figure 16: Visual damages occurred in Specimen 2 with additional of three reinforcement bars starting from 1% to 3% drift under vertical cyclic loading; (a) some diagonal minor cracks occurred in column and beam-column interfaces; (b) surface cracks occurred on reinforced concrete beam; and (c) spalling of concrete cover on front surface of column.

(a) (b) (c)

Figure 17: Minor damages occurred in Specimen 3 with additional of cross-bracing in the joint; (a) no cracks at beam-column interface at 0.2% drift; (b) diagonal crack at bottom column; and (c) diagonal and top diagonal cracks in the column and beam.

has minimum damage and crack as compared to the other two types of connection. Only hairline cracks were observed on top surface of he connections and no spalling of concrete occurred either at top or bottom of the connection. It can be concluded that the vertical cyclic load are transferred to the column through the cross-bracing of reinforcement bars in the joints. Therefore, it is suggested that cross-bracing connection should be adopted in current code of practice to avoid the damage of beam-column connection under long distant-earthquake excitation.

8.0 Experimental Results And Analysis

Figure 18 shows the hysteresis loops for load versus displacement measured using linear potentiometers marked as LVDT 1 and LVDT 2 for beam-column connection which designed according BS 8110 without additional reinforcement bars in the joints. Initially, the beam-column connections behave linearly and then non-linearly. Figure 18(a) shows hysteresis loop for LVDT 1 which placed at end of beam with maximum load of 30kN and displacement of 55mm. Figure 18(b) shows the hysteresis loop for LVDT 2 located at the center of beam. It seem that the lower part of hysteresis loop has less value of load and displacement because the foundation beam is not properly clamped to the strong floor and during testing the foundation beam did not stay stationary and it also moving upward and downward. The darker line represents the theoretical value of load versus displacement using the eight steps of moment-rotation and equations in Section 3. There are closed relationship between the theoretical values and experimental values of beam-column joints.

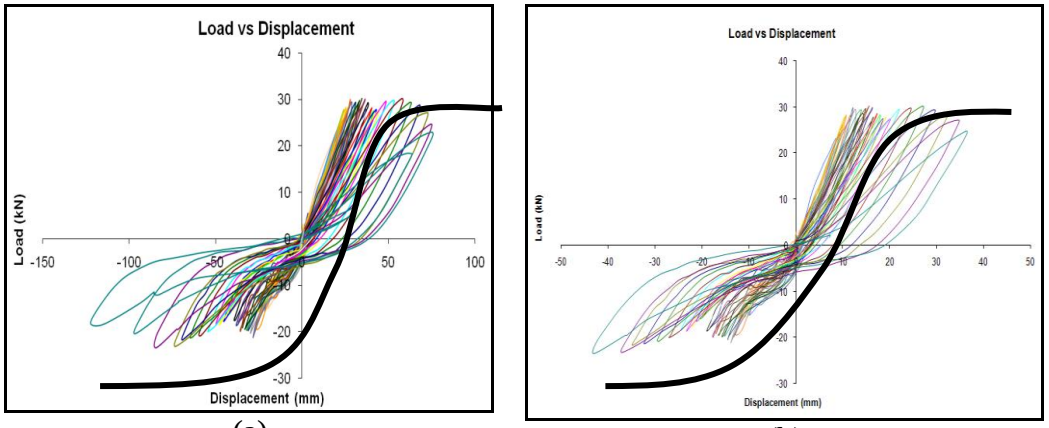

(a) (b)

Figure 18: Hysteresis loops of beam-column connection located on Specimen 1; (a) hysteresis loops for LVDT 1 and (b) hysteresis loops for LVDT 2.

Figure 19 shows the experimental and theoretical values of hysteresis loops (load versus displacement) for beam-column connection with three anchorage bars at top of beam and connected to bottom of column. The red line represents the theoretical values of load versus displacement and the blue lines correspond to the experimental values of the hysteresis loops of beam-column interface under vertical cyclic loadings. Figure 19(a) shows the hysteresis loops for LVDT 1 closed to the load cell. There some discrepancies between theoretical value and experimental value in terms of load and displacement. One of the main reasons is that while applying the vertical cyclic loading on the beam, the column is moving and it is not proper clamping to the strong floor. While the beam is moving, the column is also moving with the same direction between them. In order to get the best fit line, only the beam is allows to move while the other structures components such as beam and foundation must be in the stationary position. Figure 19(b) shows the hysteresis loops for LVDT 2 which located 500mm from LVDT 1. Both of these figures show how much energy dissipated during ground shaking. The hysteresis loops are closed to each other because the foundation beam is not properly clamped to strong floor.

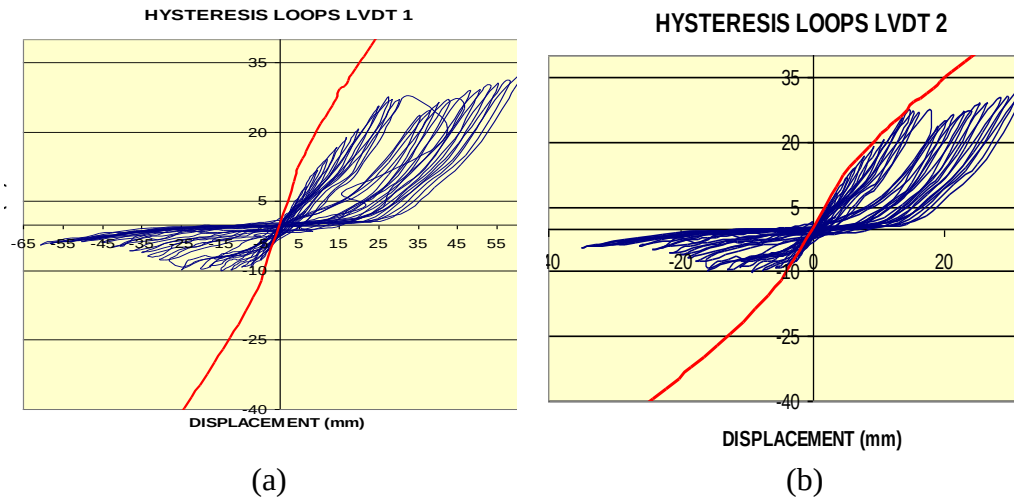

(a) (b)

Figure 19: Hysteresis loops for Specimen 2 with three anchorage bars ; (a) hysteresis loops for LVDT 1; and (b) hysteresis loops for LVDT 2.

Figure 20 shows experimental results and theoretical result of hysteresis loops (load versus displacement) of beam-column interface with additional cross-bracing reinforcement bars. Figure 20(a) shows the hysteresis loops for LVDT 1. The black darker line represents the theoretical value and maroon lines

correspond to the experimental results. Both graphs show a close relationship between them with very minimum percentage differences. Figure 20(b) shows the hysteresis loops (load versus displacement) for LVDT 2 with theoretical and experimental results. From these graphs it shows that this type of joint has higher strength capacity which is 45kN than the connection which designed according to BS 8110 which is only 32kN. These graphs are stiffer than the graph as shown in Figure 3.20 where beam-column joints as designed according to BS 8110. In other words, this type of connection can resist higher seismic loading with maximum displacement of 60mm. Therefore, it can be concluded that additional cross-bracing reinforcement bars in beam-column interfaces contribute to better stiffener, high ductility and more stability. Additional bars and cross-bracing anchorage reinforcement bars can also increase the strength and shear capacity of the connections and simultaneously improved the seismic performance of the system.

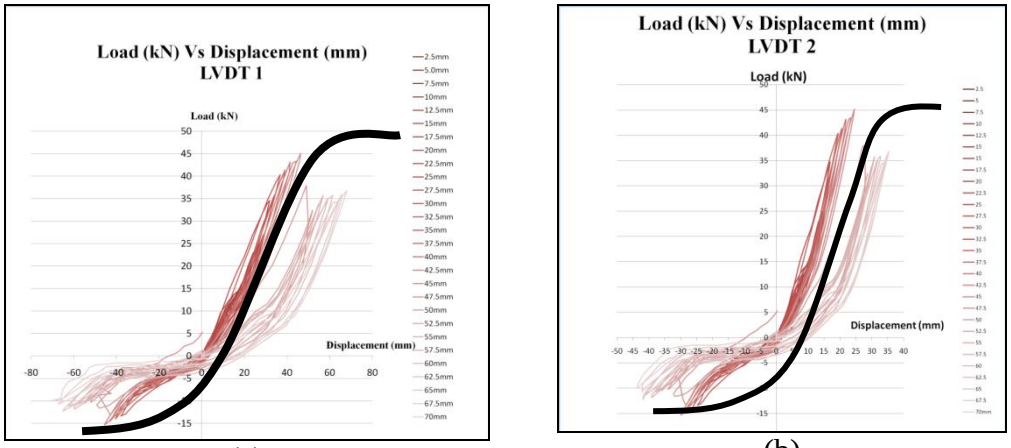

(a) (b)

Figure 20: Hysteresis loops for Specimen 3 with cross-bracing reinforcement bars; (a) hysteresis loops for LVDT 1 and (b) hysteresis loops for LVDT 2.

9.0 DISCUSSION

The seismic performance of beam-column joints under quasi-static vertical cyclic loading depends on a few parameters such as the arrangement of reinforcement bars especially at the joints, the percentage of reinforcement bars, concrete cover, compressive strength and confined concrete. These parameters have a significant effect on energy absorption, equivalent viscous damping, the base shear, shear strength, moment resistance, stiffness and ductility of beam-

column joints. The amount of energy absorbed during earthquake can be measured by determine the equivalent viscous damping of the system. The percentage of equivalent damping can be calculated by dividing the area under the hysteresis loop (load versus displacement) over average area under maximum strength in forward and reverse loading directions. Figure 21 shows graph in terms of percentage equivalent viscous damping for three different types of joints which denoted as Specimen 1, Specimen 2 and Specimen 3. Specimen 1 absorbed a lot of energy as compared to Specimen 2 and Specimen 3. It is meaning to say that Specimen 1 suffered a lot of damage, followed by Specimen 2 and finally Specimen 3. The first cycle of Specimen 1 has the greatest percentage equivalent viscous damping which is 14.78% as compared to the second cycle (12%). In earthquake, the first strike will destroy most of the buildings, infrastructures and lifeline as compared aftershock. Normally, the first strike of earthquake released a lot of energy and this energy will destroy and damage the buildings and infrastructures as compared to aftershock.

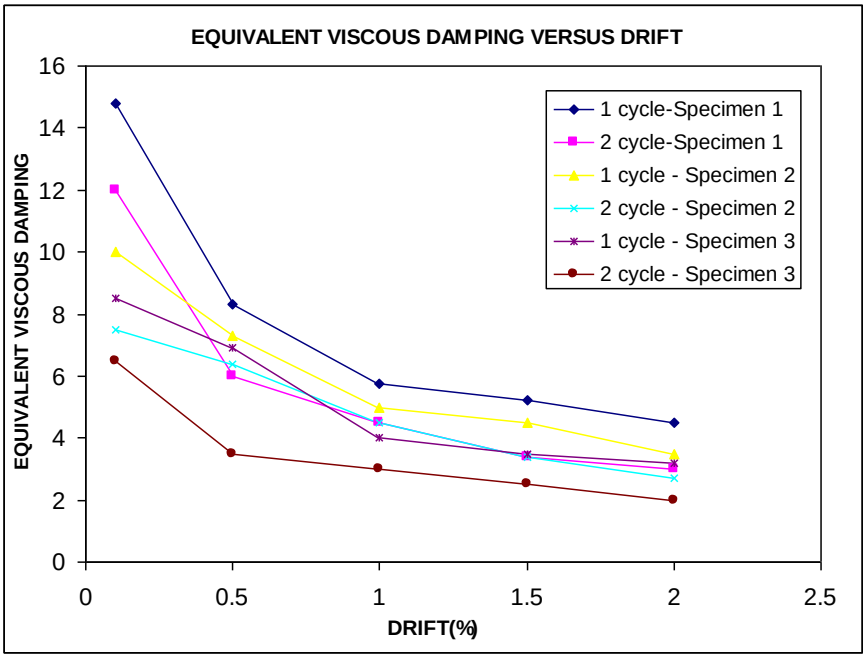

Figure 21: Equivalent viscous damping versus drift for Specimen 1, Specimen 2 and Specimen 3 at 1 cycle and 2 cycle under vertical cyclic loading.

Table 1 shows the experimental result for maximum loading and displacement for Specimen 1, 2 and 3. Based on the experimental results, the beam-connection which designed using cross-bracing reinforcement bars has the highest maximum loading capacity which is 45kN as compared to conventional method (34kN) and overlapping (30kN). It is evident that the specimen possessed bracing connection type in beam-column joint recorded the highest maximum loading capacity among the three samples. Overlapping samples has recorded the lowest maximum loading capacity during the experiment. It is observed that overlapping sample has recorded the highest deflection reading in y-axis direction (LVDT 1, 2, and 3). Hence, it is reveals that the overlapping type is less effective connection of beam-column joint among the three samples that had tested in the laboratory. Therefore, it can be concluded that the bracing joint of the beam-column connection is the greatest type of connection among the three samples of connection since it showed the well performance under seismic condition.

Table 1: Summary of experimental results on the three types of connections

LVDT No.	**Connection Type**	**Max Deflection (mm)**	**Max load (kN)**
	Conventional	63	34
1	Overlapping	75	30
(y-axis)	Bracing	70	45
	Conventional	32	34
2	Overlapping	36	30
(y-axis)	Bracing	35	45
	Conventional	3.5	34
3	Overlapping	8	30
(y-axis)	Bracing	5.5	45
	Conventional	10	34
4	Overlapping	1.5	30
(x-axis)	Bracing	2.5	45
	Conventional	1.5	34
5	Overlapping	12	30
(z-axis)	Bracing	32	45

10. Conclusion And Recommendation

Based on visual observation, experimental results and discussion as mentioned above, the conclusion and recommendation can be drawn as follows:

1. Under seismic design, structural engineers should design adequate percentage of reinforcement bars particular at the intersection between beam-column. Sufficient anchorage length must be provided to connect the longitudinal bar in beam to the longitudinal bar in the column.
2. The joints should have adequate strength and stiffness to resist the internal forces induced by the framing members and external force like earthquake and wind loadings.
3. In order to prevent the diagonal cracking and concrete crushing, the close space closed-loop steel ties can be provided around the column bars in the joint region. It can resist the shear force, thereby reducing the cracking and crushing the concrete.
4. Based on the experimental results, the cross-bracing of reinforcement bars in the beam-column connections provided the higher loading capacity and has better seismic performance as compared to the other two types of connections.
5. It is recommended that the current code of practice BS 8110 should be changed to another seismic code of practice such as Eurocode 8 so that reinforced concrete buildings in Malaysia are safe under long-distant earthquake attack.

References

Alcocer, S. M., R. Carranza, D. Perez - Navaratte, and R.Martinez. (2002), Seismic Tests of Beam to Column Connections in a Precast Concrete Frame. *Precast Concrete Institute Journal*, V. 47:30-45.

ACI 318-05, 2005), Building Code Requirement for Structural Concrete and Commentary. ACI Committee 318, 2005, 430pp.

Dodd, L.L., and Restrepo-Posada, J.I (1995), Model for Predicting Cyclic Behaviour of Reinforcing Steel. *Journal of Structural Engineering*, ASCE, Vol 34, No.4: 433-445.

Hamid, N.H.A and Iwan Surdano (September 2006), Dynamic Response of Slender/Thin Reinforced Precast Concrete Walls Using Shaking Table. *Journal-The Institution of Engineers, Malaysia*, Vol.67, No.3:48-55.

Hanson, N.W., and Conner, H.W., (1967), Seismic Resistance of Reinforced Concrete Beam-Column Joints. *Journal of the Structural Division*, ASCE, 93:533-560.

Park, R. and Paulay, T., (1975), Reinforced Concrete Structures, John Wiley & Sons, United States of America, 758pp.

Paulay, T., Park, R. and Preistley, M.J.N. (1978), Reinforced Concrete Beam-Column Joints under Seismic Actions. *Structural Journal, ASCE Journal*, **75**:585-593.

Paulay, T., Park, R. and Preistley, M.J.N. (1992), Seismic Design of Reinforced Concrete and Masonry, John Wiley Interscience, United States of America, 768pp.

Sritharan, S., Priestley, M.J.n, Seible, F. and Igarashi, A. (1998), A Five Storey Precast Concrete Test Building for Seismic Conditions-an Overview. *Proceedings of the Twelfth World Conference on Earthquake Engineering*, Auckland, paper No: 1299.

Uma, S.R. and Meher, P.A., (2002), Seismic Behavior of Beam Column Joints in Reinforced Concrete Moment Resisting Frames, *http://www.iitk.ac.in/nicee/IITK-GSDMA/EQ31, Accessed 27 August 2007.*